Journal of Cluster Science (2019) 30:1145–1155
https://doi.org/10.1007/s10876-019-01578-9

ORIGINAL PAPER

Preparation and Characterization of Chitosan Nanocomposites Material Using Silver Nanoparticle Synthesized *Carmona retusa* (Vahl) Masam Leaf Extract for Antioxidant, Anti-cancerous and Insecticidal Application

Ramanathan Rajkumar[1] · Muthugounder Subramanian Shivakumar[2] · Sengottayan Senthil Nathan[3] · Kuppusamy Selvam[1]

Received: 5 February 2019 / Published online: 8 May 2019

Abstract
Chitosan derived silver biocomposites (CsS) were produced by green synthesis using *Carmona retusa* (Vahl) Masam aqueous leaf extract. UV–Vis spectra of synthesized CsS biocomposites showed absorption maxima at 441 nm. FESEM average particle size was 51 nm and spherical in shape. TEM images of CsS biocomposite ranged between 30 nm to 60 nm, the DLS measurement showed the size of 234.1 nm for chitosan derived AgNPs. In FTIR spectra, the C–H winding and were observed for CsS biocomposites. In addition, the elemental composition showed uniform grain boundaries as recognized by EDaX spectra. In-vitro antioxidant activity CsS biocomposites showed the ability to scavenge free radicals. Cytotoxicity analysis of CsS biocomposites on MCF-7 breast cancer cell line revealed 90% inhibition at 500 µg/ml concentration. *C. retusa* mediated synthesis AgNPs coated chitosan biocomposite showed strong larvicidal activity with low LC_{50} and LC_{90} values against the malarial vector, *An. stephensi*, *Ae. aegypti*, and *Cx. quinquefasciatus* respectively. Eight bioactive components were present in aqueous leaf extracts of *C. retusa*. Based on this study we suggest that *C. retusa* plant mediated AgNPs chitosan derived silver biocomposites (CsS) has anti-cancerous and insecticidal activity which can further be explored for commercialization.

Keywords *Carmona retusa* · Chitosan · Nanoparticles · Anticancer · Insecticidal

Introduction

Nanomaterials today have several applications in pharmaceutical, cosmetic paints, displays board, batteries, catalyst, sensor, food, agricultural and construction industries [1]. Nanomedicine is an upcoming field that holds potential in an improvement of human health [2]. There are several nanomaterials which are available today which includes metals, and biopolymers. Among biopolymers, chitosan (CS) is increasingly used for biomedical application [3]. Nowadays nanocomposites having nanoparticles substituted in biopolymer matrices due to their physiochemical properties have been widely used as a model for drug delivery [4–7]. Among the various nanomaterials, silver nanoparticles (AgNPs) gained attention due to their exclusive biological, chemical, and physical properties, because of them sole antimicrobial properties, AgNPs are safe for several applications including drug and food [8]. Chitosan is a naturally occurring biopolymer in Chitin. Chitin is found in shells of crustacean like crabs, lobsters, prawn, and shrimps. Chitosan is biocompatible, non-toxic, has good permeability, high mechanical strength, and biodegradable, which makes chitosan an ideal biopolymer

✉ Kuppusamy Selvam
kselvampubotany@gmail.com

[1] Department of Botany, Periyar University, Salem, Tamil Nadu 636 011, India

[2] Department of Biotechnology, Periyar University, Salem, Tamil Nadu 636 011, India

[3] Sri Paramakalyani Centre for Excellence in Environmental Sciences, Manonmaniam Sundaranar University, Alwarkurichi, Tamil Nadu 627 412, India

for application in biomedical, pharmaceutical, biosensor, textile, and wastewater treatment [9, 10].

Carmona retusa (*Ehretia microphylla* Lam.) is a flowering plant belonging to Boraginaceae family. This plant possesses several important medicinal properties in an indigenous scheme of medicine [11]. *C. retusa* (Vahl) Masam leaf extracts are used in treatment of cough and stomach ache, root as antidote [12]. In recent years the search for natural bioactive compounds rich in antimicrobial, antioxidant, insecticidal properties and anti-inflammatory properties [13–15]. The transmission of several diseases like malaria, dengue fever, zika viral disease, filariasis, and Japanese encephalitis [16] caused by mosquitoes. Mosquito control using chemical insecticides is becoming slowly ineffective due to development of insecticide resistance. Several alternative approaches have been studied which include the use of fungal conidial suspension, fungal culture filtrates, nematicidal and metabolites from plants [17, 18]. The plant metabolites have their effectiveness which constrained by relatively large doses which are required for effective control of mosquito larvae. Nanomaterials like chitosan and metal nanoparticles like silver offer approaches which could greatly increase the effectiveness of these biopesticides. One such approach is the green synthesis of silver nanoparticles (AgNPs) [19], and coating it with chitosan polymer. These chitosan silver nanocomposites with bioactive molecules can provide targeted delivery of the drugs [20].

The present study explores the potential of *C. retusa* mediated chitosan derived silver biocomposite (CsS) for their in vitro antioxidant activity, anticancer activity on MCF-7 breast cancer cell lines and larvicidal activity.

Materials and Methods

Plant Collection

Carmona retusa (Vahl) Masam (Boraginaceae) leaves were collected from Salem district, Tamilnadu, India and taxonomic identification (No. BSI/SRC/5/23/2016/TECH/770) made by Botanical Survey of India, Coimbatore, Tamil Nadu, India.

Preparation of Chitosan Coated Silver Biocomposites

Ten gram of *C. retusa* leaf powder dissolved in 100 ml double distilled water and boiled at 50–60 °C for 10 min. A leaf decoction solution was filtered using a Whatman No. 1 filter paper. After that, 0.01 M of silver nitrate salt dissolved in 100 ml of *C. retusa* leaf extract. This aqueous silver ion mixed leaf extract the solution was continously stimulated in 80 °C temperature for six h. A brown color formed a few minutes later, following continuous stirring. The precipitate was obtained by centrifuging at 10,000 rpm for 10 min. an equal volume of chitosan in 10 ml of double distilled water was added to the precipitate and was stirred at 80 °C for 24 h. This homogeneous mixed solution was refluxed at room temperature for 24 h. Chitosan derived silver colloidal solution were centrifuge at 15,000 rpm for 10 min to precipitate out the CsS biocomposites.

Characterization Techniques

CsS biocomposites characterized by X-ray diffractometer (model: X'PERT PRO PANalytical). Samples, the diffraction patterns were recorded via the range of 20°–80°. Where the monochromatic wavelength of 1.54 Å was used. FT-IR spectra were recorded from 400 to 4000 cm^{-1} using a Perkin-Elmer spectrometer. Absorption spectra of CsS biocomposites were studied via the range among 200 and 800 nm by Lambda 35 spectrometer. Field Emission Scanning Electron Microscopy (FESEM with EDaX) using Carl Zeiss Ultra 55 Inca model used for the surface morphological analysis of AgNPs. Transmission electron microscopy analysis, (PHILIPS, CM 200, Operating voltages: 20–200 kv Resolution: 2.4 Å) was used to identify the size and morphology of the prepared CsS biocomposites. Selected Area Electron Diffraction pattern (SAED) was used to evaluated phase structure and crystallinity of prepared nanoparticles.

Antioxidant Activity

DPPH Radical Scavenging Activity (2,2-Diphenyl-1-picrylhydrazyl)

Toxicity of CsS biocomposites for scavenging DPPH radical activity was done followed by Molyneux et al. [21] with slight modification. Percentage of inhibition calculated using (Absorbance of control − Absorbance of the test)/Absorbance of control) × 100. The calculated IC_{50} value by GraphPad PRISM 5.0.

Hydrogen Peroxide Radical Scavenging Activity (H_2O_2)

Hydroxyl Peroxide radical scavenging capacity of pure Zinc Oxide and alkaline metal ions (Mg, Ca, Sr and Ba) doped with Zinc Oxide nanoparticles were determined according to Halliwell et al. [22].

In-Vitro Anticancer Activity

MCF-7 human breast cancer cell-line procured from the National Center for Cell Science (NCCS), Pune, India. All experiments performed on cells from passage 15 or less. CsS biocomposites suspended in dimethyl sulfoxide (DMSO), to prepare a stock solution and further, the solution was diluted with media to get different concentrations. 200 µl of CsS in different concentration added to wells containing 5×10^3 MCF-7 cells per well. The control treated with DMSO solution. After 24 h, 20 µl of MTT solution (5 mg/ml in PBS) added to both well, and the plate was covered with aluminum foil and incubated for four h at 37 °C [23]. Purple formazan outcome was dissolved by adding 100 µl of DMSO in both well. In 96-well plate reader (Bio-Rad, iMark, USA) absorbance was read at 570 nm (measurement) and 630 nm (reference). Three replicates used for the experiments and data were calculated by the particular significance. The percentage of inhibition calculated from the relation:

$$\frac{mean\ OD\ of\ untreated\ cells\ (control) - mean\ OD\ of\ treated\ cells}{mean\ OD\ of\ untreated\ cells\ (control)} \times 100$$

Mosquito Culture

Eggs of *Aedes aegypti*, *Anopheles stephensi* and *Culex quinquefasciatus* were obtained from the Institute of Vector Control Zoonoses (IVCZ), Hosur and maintained separately in a plastic tray which containing tap water and 75–85% relative humidity under photoperiod cycles in 14:10 (Light and Dark). Each larva was fed with an equal quantity of dog biscuits, yeast powder, and millet powder as 3:1:3 ratio.

Larvicidal Activity of CsS Biocomposites

Larvicidal activity was studied by the standard procedure recommended by World Health Organization [24]. Green synthesized CsS biocomposites were dissolved in 1 ml of distilled water and prepared into various concentrations viz, 100, 200,300,400 and 500 ppm with double distilled water. Twenty-five fourth instar larvae from each concentration transferred in 500 ml beakers, and the experiment performed in three replicates under the laboratory condition. Larval mortality observed at 24 h of the exposure period. During both exposure periods, no food supplied to the larvae. Percentage of mortality was calculated and was corrected using Abbott's formula [25].

Data Analysis

The larval mortality data subjected to Probit analysis for calculating LC_{50}, LC_{90}, and other statistics using the SPSS 16.0.

GC–MS Analysis of *C. retusa* Leaf Extract

Gas chromatography–mass spectrometry analysis was performed using GC Clarus 500 (Perkin Elmer), carrier gas used Helium, Column lite-1 (100% Dimethyl polysiloxane), 30 × 0.25 mmx, 1 ml per min, split: 10:1 Mass detector turbo mass gold-Perkin Elmer, Mass detector: Turbo mass gold-Perkin Elmer. 2 µl of the sample injected, and it ran for 36 min at 250 °C. The MS NIST library used for the identification of the compounds.

Results and Discussion

Synthesis and Characterization

The mediated synthesis of chitosan derived silver bio composites (CsS) were produced from *C. retusa aqueous* leaf extract. UV–Vis absorption spectrum of synthesized CsS biocomposites absorption maxima at 441 nm (Fig. 1). Prominent peak ranges between 410 and 450 nm are ascribed to Surface Plasmon Resonance (SPR) of AgNPs in particles size ranging from 25 to 50 nm [26]. From the literature, the SPR in the area of approximately 410–450 nm is attributed to sphere-shaped nanoparticles [27]. X-ray diffraction was used to analyze the crystalline

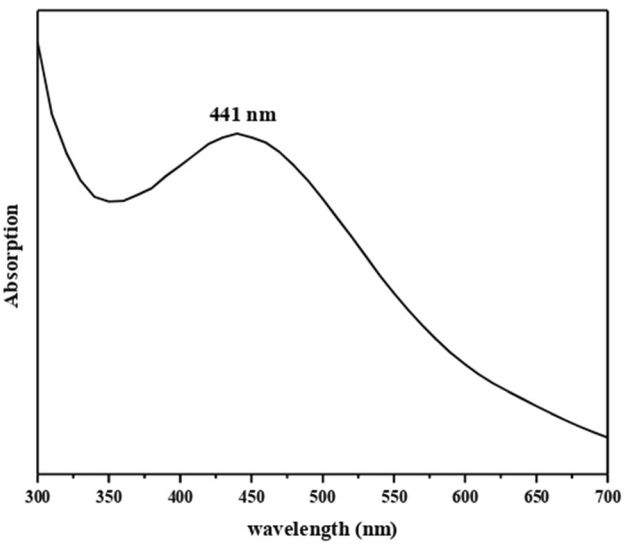

Fig. 1 UV–Vis absorption spectra of CsS biocomposites (*C. retusa* derived AgNPs + Chitosan) UV–Vis absorption spectrum of synthesized CsS biocomposites absorption maximum at 441 nm

phase of CsS biocomposites synthesized with *C. retusa* leaf extract (Fig. 2). XRD peaks situated at angle 38.1144, 44.3321, 64.4215 and 77.3487 matching with (111), (200), (220) and (311) planes of CsS for the face-centered cubic silver as per the JCPDS card no. 89-3722 [28].

The lattice constants 'a' of the cubic structure of CsS biocomposites was calculated *by* using the formula.

$$\frac{1}{d^2} = \left(\frac{h^2 + k^2 + l^2}{a^2}\right) \quad (1)$$

The lattice constant 'a' is received through the relation $a = \sqrt{d^2(h^2 + k^2 + l^2)}$. The calculated 'a' value is 4.0897 Å for CsS biocomposites.

The average crystallite sample size is calculated by using the XRD pattern according to Debye–Scherrer's relation

$$\text{Average crystallite size } D = \frac{k\lambda}{\beta_{D\cos\theta}} \quad (2)$$

where λ is the radiation wavelength (1.54056 Å for CuKα radiation), k is a constant, which is the same to 0.94, β is the peak width at half-highest intensity, θ is the peak at the position. The standard crystallite size was found to be 34.16 nm CsS biocomposites. FT-IR spectroscopic analysis reveals vibrational frequencies of CsS biocomposites (Fig. 3). The peak at 3020–3650 cm^{-1} was found to be O–H bonds. From the IR result, the O–H stretching band is raised at 3167 cm^{-1} for CsS biocomposites. The peaks at 2923 cm^{-1} are owing to symmetric and asymmetric C–H stretching. The amine group is raised at 1572 cm^{-1} corresponding to N=O Nitroso for chitosan functional groups. From the FT-IR spectra, the $–CH_3$ alkenes and C–F

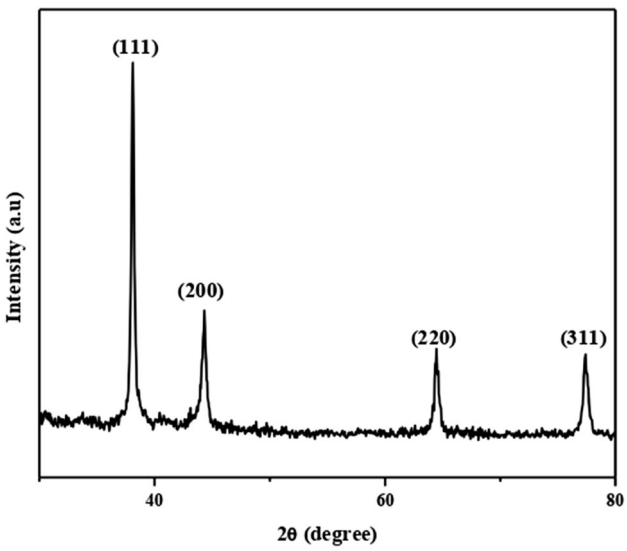

Fig. 2 X-ray diffraction (XRD) pattern of CsS biocomposites (*C. retusa* derived AgNPs + Chitosan). The standard crystallite size was found to be 34.16 nm CsS biocomposites

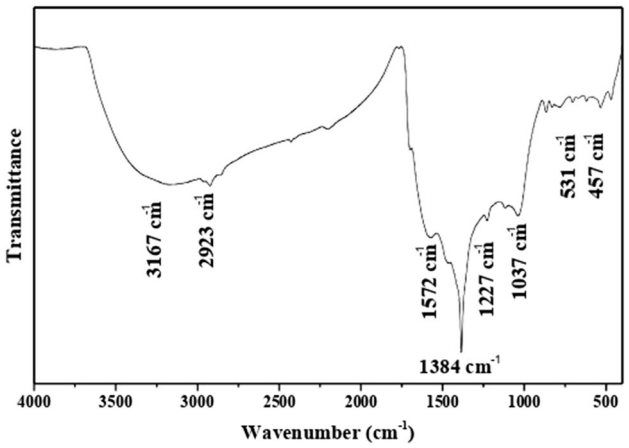

Fig. 3 Fourier-transform infrared spectroscopy (FT-IR) spectral analysis of CsS biocomposites (*C. retusa* derived AgNPs + Chitosan). Peak at 3020–3650 cm^{-1} was found to be the reason for vibrational method of the O–H bonds

stretching Alkyl halides observed at 1384 and 1227 cm^{-1} for CsS biocomposites. Therefore, the major phytochemical present in the leaf extract of *C. retusa*. Responsible factor for the raised reduction and capping is bioactive components, and it is during the synthesis of CsS biocomposites. The S–S Disulfide asymmetric bonding and C–Br stretching alkyl halides stretching are originated to be 531 and 457 cm^{-1} for CsS biocomposites. The C–H bonding peak increases due to the conversion of $AgNO_3$ to AgNPs [29]. Similarly Wei et al. [30] reported that the chitosan-based silver nanoparticles showed strong amine group ($–NH_2$) that can be electrostatically interact with Ag^+ ions adsorbed on the surface of silver nanoparticles. Further, bands observed at 1418 cm^{-1} assigned with vibration of –OH group and 1373 cm^{-1} symmetric assigned with CH_3 (alkenes).

FESEM images of CsS biocomposites exhibits nanosheet mediated sphere-shaped nanoparticles with uniform grain boundaries (Fig. 4a). The average particles size was 51 nm for CsS biocomposites. From the EDaX analysis showed the maximum indication of weight percentage of Ag (43.25%) followed by O (36.94%), and K (11.23%), respectively for CsS biocomposites (Fig. 4b). TEM images revealed that the prepared hybrid chitosan derived silver nanoparticles were spherical in shape and size ranged between 30 nm to 60 nm (Fig. 5a, b and c), SAED pattern of hybrid Chitosan derived silver nanoparticles showed high crystalline nature of the extract, due to its corresponding well-pronounced Debye–Scherrer diffraction rings in the selected area electron diffraction (SAED) pattern (Fig. 5d) that can be assigned to the reflections (1 1 1), (2 0 0), (2 2 0) and (3 1 1) of cubic AgNPs. There were no additional rings in the SAED pattern stemming from

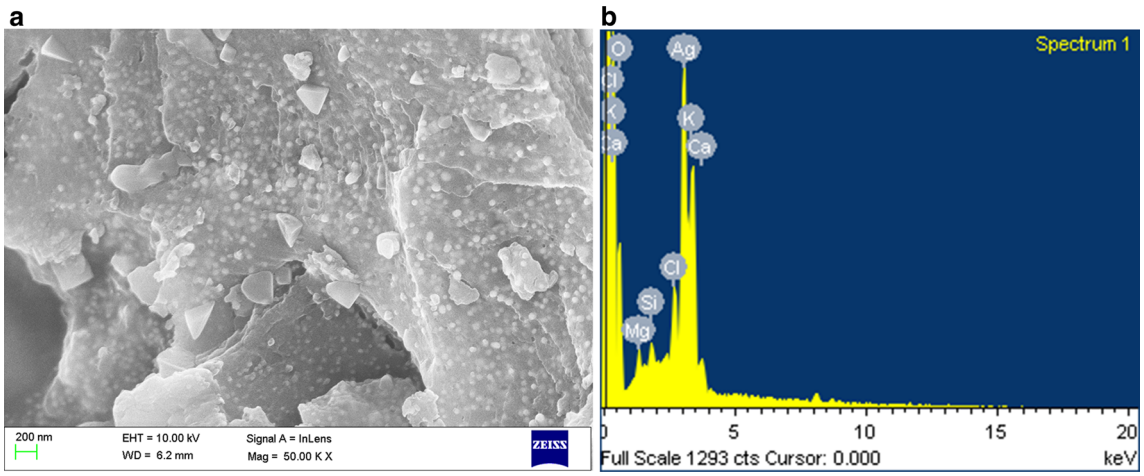

Fig. 4 **a** Field emission scanning electron microscope (FESEM) image of CsS biocomposites (*C. retusa* derived AgNPs + Chitosan). FESEM images of CsS biocomposites exhibits nanosheet mediated sphere-shaped nanoparticles with uniform grain boundaries and average particles size was 51 nm for CsS biocomposites. **b** EDaX spectra of CsS biocomposites (*C. retusa* derived AgNPs + Chitosan). EDaX analysis showed the indication of Ag, O and K weight percentage are 43.25%, 36.94% and 11.23% for CsS biocomposites

any crystalline impurities. The DLS measurement showed the size of 234.1 nm for chitosan derived AgNPs (Fig. 5e).

In-Vitro Antioxidant Activity

The equilibrium between antioxidant and oxidation is supposed to be a large factor in maintaining a healthy biological system [31]. In current years, a lot of studies reported that the importance of free radical scavenging and reactive oxygen species (ROS) in the etiology and progress of many human diseases [32, 33] ROS are involved in damage to DNA, cell membranes, cellular proteins, and induce cell death. They are produced as a result of toxicant exposure to the cells; two of the most important ROS are O_2 radical and OH radical [34]. Such reactions will most likely dominate the recombination of two $^{\bullet}OH$ radicals to appearance hydrogen peroxide. Superoxide anion radical ($^{\bullet}O_2^-$), on the further hand, inadequately permeates to cell membranes and found less toxic nature [35, 36]. Hydrogen peroxide is as well measured to be the weaker oxidizer, other than it could cause cell damage via hydroxyl radicals which are formed from the Fenton reaction [37, 38]. Also, H_2O_2 with the presence of ($^{\bullet}O_2^-$) can produce singlet oxygen, that is extremely toxic, are of the maximum biological significance. In some intracellular systems, ROS are produced continuously in all cells, whereas metabolic by-products. However, this method requires metal or another catalyst [39].

$$^{\cdot}O_2^- + H_2O_2OH^- + OH^{\cdot} + {}^1O_2$$

In living systems, free radicals are produced due to an interaction of biomolecules with molecular oxygen [39, 40] these free radicals are accountable for the degradation of biomolecules. Oxidation is also responsible for nutritional quality deterioration and discoloration of food [41]. Lipid peroxide and low molecular weight compound are generated as a result of consumption of oxidized foods which results in damage to cell membranes leading to death. Antioxidants play a significant role in scavenging of this toxic free radical in the biological system [42, 43]. So far, several kinds of natural and synthetic antioxidants had been investigated for their ability to reduce the damage caused by ROS. Earlier studies have reported that the nanostructured materials are capable of free radical scavenging which are better than their heavier counterparts. This feature is owing to the high surface to volume ratio of the nanostructures [44].

The present results show that the concentrations ranging from 20 to 100 µg/ml of CsS biocomposites on DPPH, and H_2O_2 radical scavenging activity show a dose-dependent increase (Fig. 6; Table 1). DPPH radical scavenging solution contains both π system and an unpaired electron in nitrogen atom. Substitution on aromatic ring increases the molar absorptivity, and the effect becomes important when the substituent increase conjugation length take place. The complete conjugation regularly causes shifted in the benzene absorption bands from shorter to a longer wavelength. The peak at 517 nm is responsible for $n \rightarrow \pi^*$ energy transition. DPPH radical scavenging solution gradually the color changes from deep violet to pale yellow (Fig. 6). DPPH radical scavenging activity was increasing with the increasing concentration of CsS biocomposites, this result shows the CsS biocomposites scavenging free radical formation again. At level from 20 to 100 µg/ml, CsS biocomposites showed a scavenging rate ranging from 12.89 to 76.38% and IC_{50} concentration at 55 µg/ml. The above-

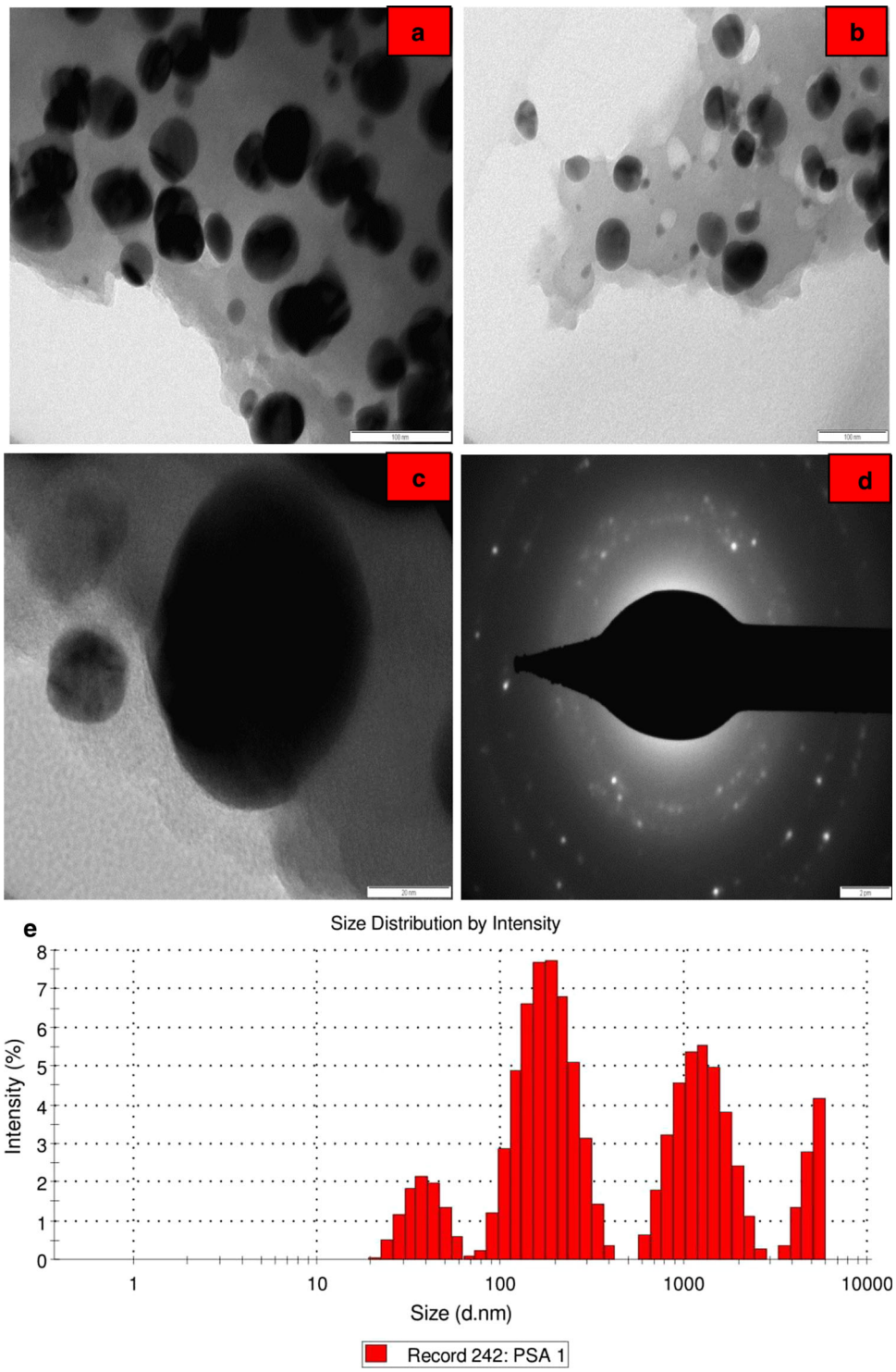

Fig. 5 Transmission electron microscopy (TEM) **a**, **b** and **c** of CsS biocomposites (*C. retusa* derived AgNPs + Chitosan) TEM images revealed that the prepared hybrid chitosan derived silver nanoparticles were spherical in shape and size ranged between 30 to 60 nm analysis and **d**. Selected Area Electron Diffraction pattern (SAED) image of CsS biocomposites (*C. retusa* derived AgNPs + Chitosan). **e** DLS measurement showed the size of 234.1 nm for CsS biocomposites (*C. retusa* derived AgNPs + Chitosan)

observed activity was lower than that of the average Ascorbic Acid (38.5 to 90.6) and IC_{50} concentration at 36 µg/ml (Table 1 and 2). Antioxidant activity of CsS biocomposites may be due to the transfer of electron pressure located at oxygen to the odd electron located at nitrogen atom in DPPH resulting the increase inhibition of $n \rightarrow \pi^*$ transition at 517 nm.

H_2O_2 radical scavenging activity power determined by its ability to convert H_2O_2 into the water. The volume of H_2O_2 scavenging activity is a useful method for determining the capability of antioxidants to decrease the level of pro-oxidants. H_2O_2 is a weak oxidizing agent which inactivates enzymes by oxidizing the essential thiol (–SH) groups of proteins. H_2O_2 readily penetrates cell membranes

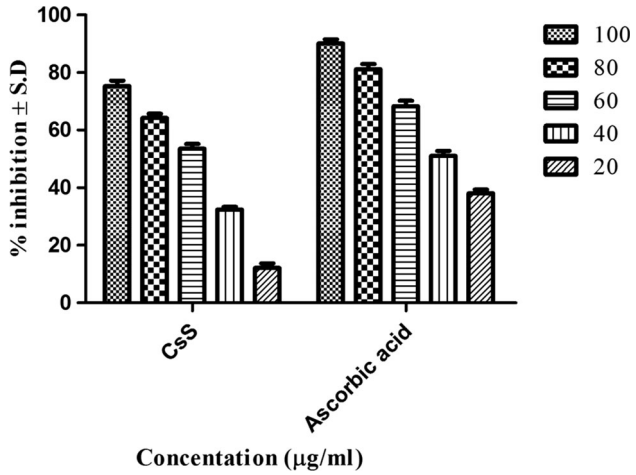

Fig. 6 DPPH radical scavenging activity of CsS biocomposites (*C. retusa* derived AgNPs + Chitosan). CsS biocomposites showed a scavenging rate ranging from 12.89 to 76.38% and IC_{50} concentration at 55 µg/ml (not significant, $p > 0.05$)

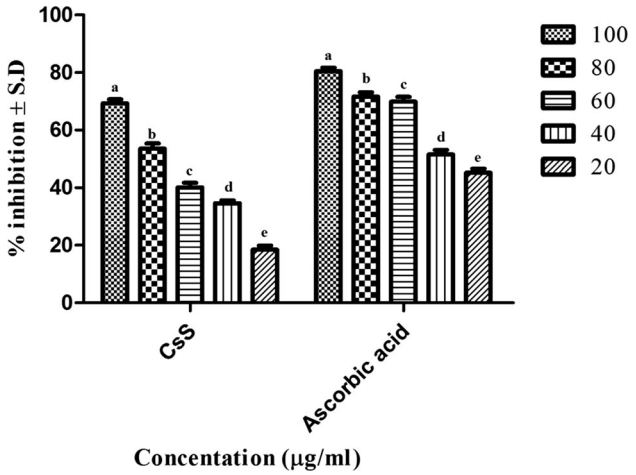

Fig. 7 H_2O_2 radical scavenging activity of CsS biocomposites (*C. retusa* derived AgNPs + Chitosan). H_2O_2 radical scavenging activity increased with dose depend manner of CsS biocomposites, this result shows the CsS biocomposites scavenging again free radical formation (not significant, $p > 0.05$)

and inside the cell, reacts with Fe^{2+} to show the hydroxyl radical activity, which exerts adverse effects [45]. The mixture of reduced iron and H_2O_2 gives $OH^{\bullet}$ is well-known. Effect of CsS biocomposites on scavenging of H_2O_2 free radical shown in Fig. 7 and Table 2. The H_2O_2 radical scavenging activity was increasing with the increasing concentration of CsS biocomposites; this result shows the CsS biocomposites scavenging free radical formation again. At concentrations 20 to 100 µg/ml, CsS

Table 1 DPPH radical scavenging activity of CsS biocomposites (*C. retusa* derived AgNPs + Chitosan). Inhibitory concentration (IC_{50})

Group	Concentration (µg/ml)	% of Inhibition	IC_{50} value
CsS biocomposites	100	76.38 ± 0.6	55 µg/ml
	80	64.82 ± 1.1	
	60	54.43 ± 0.2	
	40	33.54 ± 1.3	
	20	12.89 ± 4.0	
Ascorbic Acid	100	90.6 ± 0.5	36 µg/ml
	80	81.9 ± 3.2	
	60	69.3 ± 2.7	
	40	52.0 ± 6.4	
	20	38.5 ± 5.5	

Table 2 H_2O_2 radical scavenging activity of CsS biocomposites (*C. retusa* derived AgNPs + Chitosan). Inhibitory concentration (IC_{50})

Group	Concentration (µg/ml)	% of Inhibition	IC_{50} value
CsS biocomposites	100	69.25 ± 3.68	74 µg/ml
	80	53.52 ± 0.60	
	60	40.15 ± 2.05	
	40	34.59 ± 1.29	
	20	18.48 ± 1.59	
Ascorbic Acid	100	80.48 ± 0.5	37 µg/ml
	80	71.63 ± 1.3	
	60	66.90 ± 0.9	
	40	51.56 ± 1.0	
	20	45.20 ± 0.4	

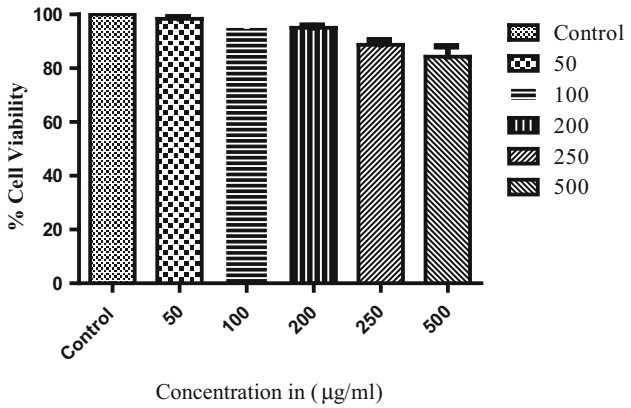

Fig. 8 Cell viability decreased with dose depend manner of CsS biocomposites (*C. retusa* derived AgNPs + Chitosan) treated with MCF-7 human breast cancer cell line (not significant, $p > 0.05$)

biocomposites showed as rate ranging from (18.48 to 69.25%) IC_{50} concentration at 74 µg/ml. The average ascorbic acid inhibition values are (45.20 to 80.48%) and IC_{50} concentration at 37 µg/ml.

In Vitro Anticancer Activity

CsS biocomposites are essential as model drug delivery systems, due to their non-toxic nature [46]. In our result, the cytotoxicity studies carried out using CsS biocomposites on MCF-7 for human breast cancer cell lines demonstrate the direct dose–response (Fig. 8). CsS biocomposites prepared using green synthesis produced 90% inhibition at the highest concentration (500 µg/ml) (Fig. 9a–f). Cell viability percentage partially decreased with the increasing level of CsS biocomposites.

Larval Bioassay

CsS biocomposites show strong larvicidal activity with low LC_{50} and LC_{90} values in *An. stephensi*, 84.600 and 274.114 ppm; *Ae. aegypti*, 86.993 and 329.306 ppm and *Cx. quinquefasciatus*, 60.581 and 229.809 ppm respectively (Table 3).

GC–MS analysis of *C. retusa* aqueous leaf extract showed the presence of eight compounds such as, urs-12-en-24-oic acid, 3-oxo-, methyl ester (45.67%), beta-amyrin (19.20%), 9,12,15-octadecatrienoic acid (9.47%), 2r-acetoxymethyl-1,3,3-trimethyl-4t-(3-methyl-2-buten-1-yl)-1t-cyclohexanol (7.73%), eicosanoic acid, 2,3-bis [(trimethylsilyl)oxy] propyl ester (7.65%), dl-.alpha.-tocopherol (4.78%), tetratriacontane (3.19%), 3,7,11,15-tetramethyl-2-hexadecen-1-ol (2.34%) were present (Fig. 10; Table 4). Urs-12-en-24-oic acid, 3-oxo-, methyl ester and beta-amyrin these be involved in anti-cancer, and antioxidant. Previous reports strongly support to our results urs-

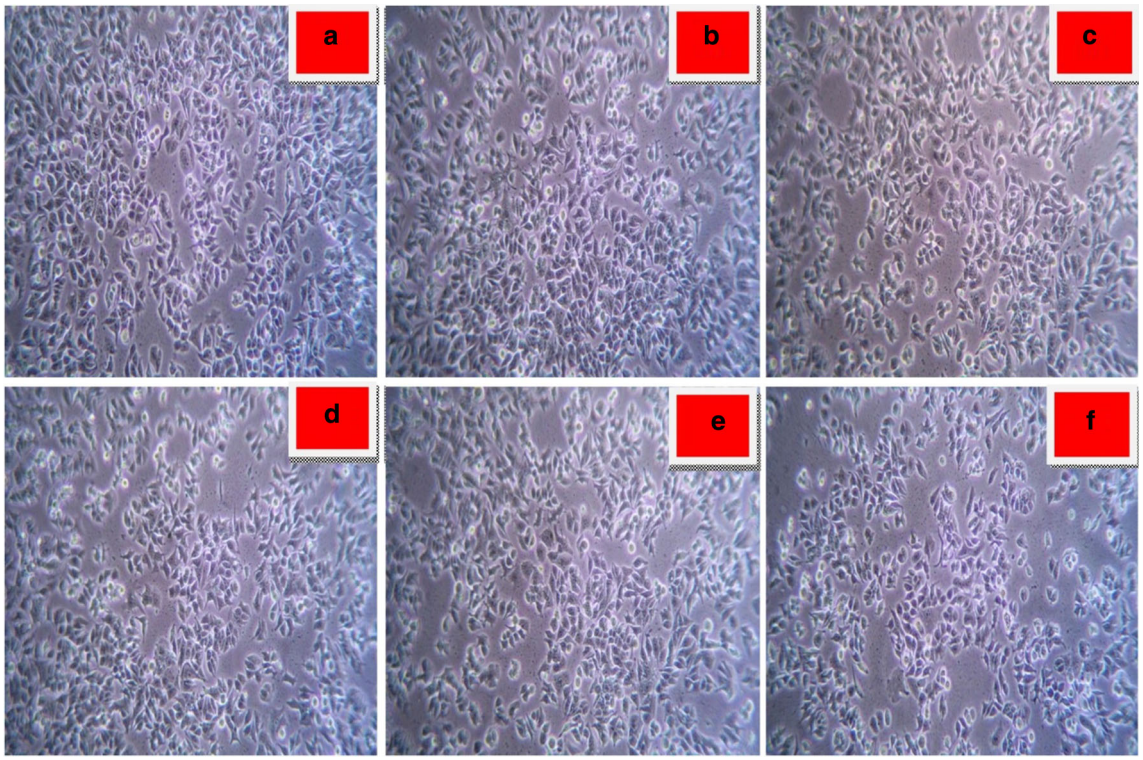

Fig. 9 Anti-cancer activity of CsS biocomposites (*C. retusa* derived AgNPs + Chitosan) **a** control, **b** 25 µg/ml, **c** 50 µg/ml, **d** 100 µg/ml, **e** 250 µg/ml and **f** 500 µg/ml concentration (10×) and cells were viewed and photographed under light microscope at 40× magnification

Table 3 Larvicidal activity of *Carmona retusa* (Vahl) Masam leaf extract and CsS biocomposites (*C. retusa* derived AgNPs + chitosan) against fourth instar of *Aedes aegypti, Anopheles stephensi* and *Culex quinquefasciatus* mosquitoes

Mosquito Species n[a] (375)	Plant	Concentration in ppm	LC_{50} (LCL-UCL) ppm	LC_{90} (LCL-UCL) ppm	χ^2	df
Ae. Aegypti	Plant Extract	100 200	791.361 (580.481–1507.341)	4020.580 (1926.309–5575.984)	0.037	3
	C. retusa derived AgNPs + Chitosan	300 400 500	86.993 (57.913–111.354)	329.306 (274.154–429.425)	1.547	3
An. stephensi	Plant Extract	100 200	575.577 (460.618–851.920)	2666.251 (1504.560–8331.222)	0.751	3
	C. retusa derived AgNPs + Chitosan	300 400 500	84.600 (15.121–132.457)	274.114 (189.374–667.586)	6.341	3
Culex quinquefasciatus	Plant Extract	100 200	473.428 (384.996–665.052)	2593.242 (2316.686–21150.792)	3.749	3
	C. retusa derived AgNPs + Chitosan	300 400 500	60.581 (45.198–115.329)	229.809 (127.231–1150.684)	7.289	3

No mortality was observed in the control

n[a] = total number of mosquitoes used per each species, 25 per replicate, three replicates were carried out, five concentrations were tested; LC_{50} = lethal concentration killing 50% of exposed organisms; LC_{90} = lethal concentration killing 90% of exposed organisms; LCL = 95% lower confidence limits; UCL = 95% upper confidence limits; χ^2 = Chi-square (n.s = not significant, $p > 0.05$); df = degrees of freedom

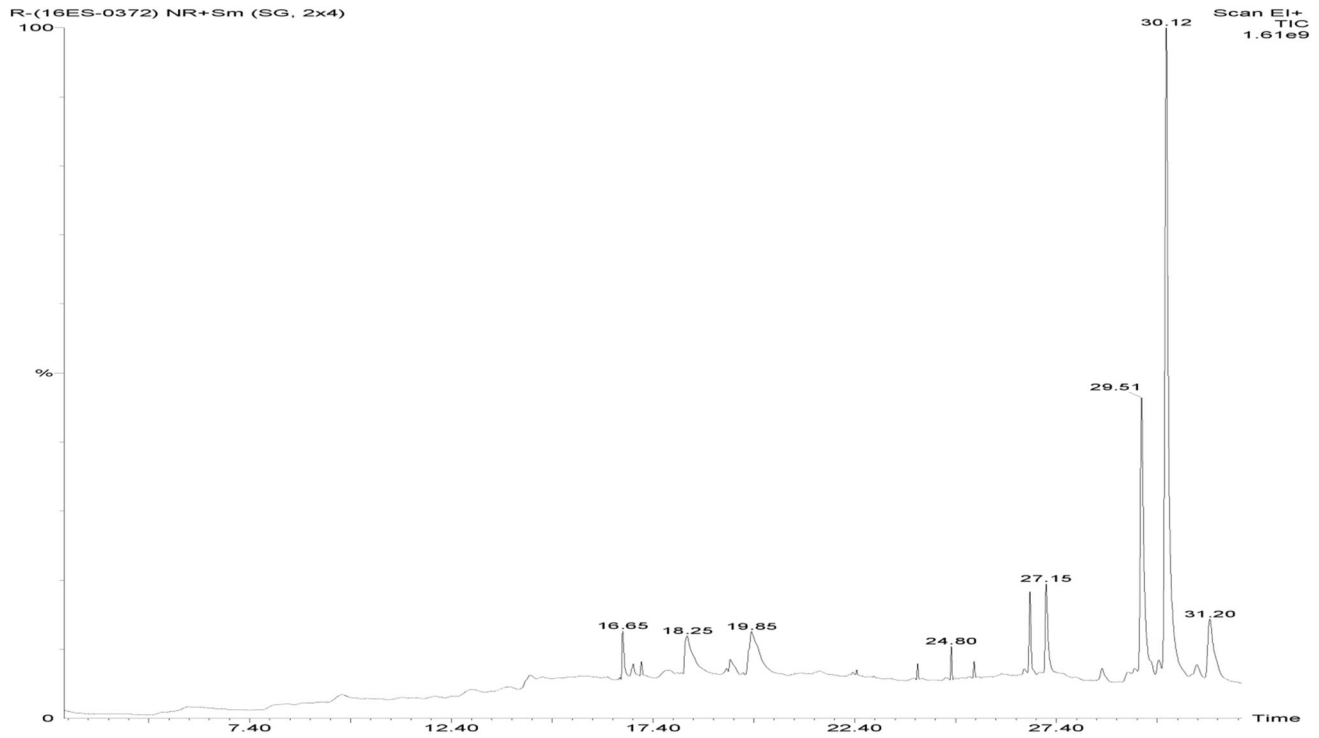

Fig. 10 Gas Chromatography and Mass Spectrum (GC–MS) Analysis of *C. retusa* aqueous extract. Urs-12-en-24-oic acid, 3-oxo-, methyl ester (45.67%) and beta-amyrin (19.20%) as a major chemical constituent may be involved in anti-cancer, antioxidant and insecticidal activities

Table 4 Gas chromatography and mass spectrum (GC–MS) analysis of *C. retusa* aqueous leaf extract

S. no.	Compound name	% of Peak area	Retention time (RT)	Molecular formula (MF)	Molecular weight (MW)S
1.	3,7,11,15-Tetramethyl-2-hexadecen-1-ol	2.343	16.64	$C_{20}H_{40}O$	296
2.	Eicosanoic acid, 2,3-bis[(trimethylsilyl)oxy]propyl ester	7.652	18.25	$C_{20}H_{40}O_2$	312
3.	9,12,15-Octadecatrienoic acid	9.476	19.84	C18H36O2	284
4.	Tetratriacontane	3.119	26.74	$C_{30}H_{62}$	422
5.	Dl-.alpha.-tocopherol	4.788	27.14	$C_{29}H_{50}O_2$	430
6.	Beta.-amyrin	19.207	29.51	$C_{30}H_{50}O$	426
7.	Urs-12-en-24-oic acid, 3-oxo-, methyl ester	45.678	30.12	$C_{31}H_{48}O_3$	468
8.	2R-acetoxymethyl-1,3,3-trimethyl-4t-(3-methyl-2-buten-1-yl)-1t-cycloh	7.737	31.20	$C_{14}H_{9O}NC_{12}$	282

12-en-24-oic acid, 3-oxo-, methyl ester and beta-amyrin are involved for antimicrobial, anti-inflammatory, anti-arthritic, diuretic and antiasthma activities [47, 48]. In addition to that, our results are accordance with earlier reports that, the compound beta-amyrin and 2r-acetoxymethyl-1,3,3-trimethyl-4t-(3-methyl-2-buten-1-yl)-1t-cyclohexanol have larvicidal activity [49, 50]. Insecticidal potential of the extract may be due to the presence of these two compounds. Further studies on isolation and characterization of these compounds can give encouraging results.

Conclusion

The importance of CsS biocomposites as an efficient system for drug delivery, antioxidant and insecticidal activity explored in the present study. CsS biocomposites give an ideal composition of being an excellent antioxidant besides having anticancerous and insecticidal potential. The size of the synthesized biocomposites as characterized by FESEM and EDaX enable the effectiveness of this composite as a potential therapeutic and an insecticidal candidate. Further studies can be done to explore the possibility of developing CsS biocomposites on a commercial scale for various biomedical applications.

Acknowledgements This research was funded by University Grants Commission-Rajiv Gandhi National Fellowship Programme (Sanction Number: F1-17.1/2016-17/RGNF-2015-17-SC-TAM-26510) for their financial support. The authors also are thankful to the Department of Botany, School of Life Sciences, Periyar University, Salem, Tamil Nadu-636 011, India, for providing infrastructural facility, and KIRND Institute of Research and Development Pvt Ltd, Tiruchirappalli, Tamil Nadu-620 020, India, for GC–MS analysis and Antioxidant studies.

Compliance with Ethical Standards

Conflict of interest The authors declare that they have no conflict of interest.

References

1. S. Arivalagan, S. Ravichandran, K. Rangasamy, and E. Karthikeyan (2011). *Int. J. Chem. Tech. Res.* **3**, 534–538.
2. M. K. Teli, S. Mutalik, and G. K. Rajanikant (2010). *Curr. Pharm. Des.* **16**, 1882–1892.
3. A. Domard (2011). *Carbohydr. Polym.* **84**, 696–703.
4. S. Cumana, J. Simons, A. Liese, L. Hilterhaus, and I. Smirnova (2013). *J. Mol. Catal. B Enzym.* **85–86**, 220–228.
5. M. Imperiyka, A. Ahmad, S. A. Hanifah, and F. Bella (2014). *Phys. B* **450**, 151–154.
6. Y. Xie, J. Zhao, Z. Le, M. Li, J. Chen, Y. Gao, Y. Huang, Y. Qin, R. Zhong, D. Zhou, and Y. Ling (2014). *Compos. Sci. Technol.* **99**, 141–146.
7. M. Catauro, F. Bollino, P. Veronesi, and G. Lamanna (2014). *Mater. Sci. Eng. C* **39**, 344–351.
8. Y. He, X. Li, Y. Zheng, Z. Wang, Z. Ma, Q. Yang, B. Yao, Y. Zhao, and H. Zhang (2018). *New J. Chem.* **42**, 2882–2888.
9. S. Sarkar, E. Guibal, F. Quignard, and A. K. SenGupta (2012). *J. Nanopart. Res.* **14**, 715.
10. N. R. Abdelsalam, A. Abdel-Mageed, H. M. Ali, M. Z. M. Salem, M. F. A. Al-Hayali, and M. S. Elshikh (2018). *Ecotoxicol. Environ. Saf.* **155**, 76–85.
11. K. C. Mouli, T. Vijaya, and S. D. Rao (2009). *Pharm. Technol.* **1**, 4–8.
12. D. L. Shrisha, K. A. Raveesha, and N. Nagabhushan (2011). *J. Med. Plants. Res.* **17**, 4087–4093.
13. R. Rajkumar, M. S. Shivakumar, S. Senthil Nathan, and K. Selvam (2018). *J. Clust. Sci.* **29**, 1243–1253.
14. Y. He, F. Wei, Z. Ma, H. Zhang, Q. Yang, B. Yao, Z. Huang, J. Li, C. Zeng, and Q. Zhang (2017). *RSC Adv.* **7**, 39842–39851.
15. S. Some, I. K. Sen, A. Mandal, T. Aslan, Y. Ustun, E. S. Yilmaz, A. Kati, A. Demirbas, A. K. Mandal, and I. Ocsoy (2019). *Mater. Res. Express.* **6**, 012001–012022.
16. G. Benelli (2015). *Parasitol. Res.* **114**, 2801–2805.
17. P. Vivekanandhan, S. Karthi, M. S. Shivakumar, and G. Benelli (2018). *Pathogens Global Health* **112**, 37–46.
18. G. Benelli and R. Pavela (2018). *Ind. Crops Prod.* **117**, 382–392.
19. G. Benelli (2016). *Parasitol. Res.* **115**, 23–34.

20. A. Anitha, S. Sowmiya, P. T. Sudheesh Kumar, S. Deepthi, K. P. Chennazhi, H. Ehrlich, M. Tsurkan, and R. Jayakumar (2014). *Prog. Polym. Sci.* **39**, 1644–1667.
21. P. Molyneux (2004). *J. Sci. Technol.* **26**, 211–219.
22. B. Halliwell, J. M. Gutteridge, and O. I. Aruoma (1987). *Anal. Biochem.* **165**, 215–219.
23. T. Mosmann (1983). *J. Immunol. Methods* **65**, 55–63.
24. WHO (2005). cds/WHO-pes/gcdpp/13.
25. W. S. Abbott (1925). *J. Ecol. Entomol.* **18**, 265–267.
26. P. Sivalingam, J. J. Antony, D. Siva, S. Achiraman, and K. Anbarasu (2012). *Colloids Surf. B Biointerfaces* **98**, 12–17.
27. A. Maniraj, S. Muthuram Kumar, M. Kannan, K. Rajarathinam, and A. Pushparaj (2017). *J. Adv. Appl. Sci. Res.* **9**, 97–106.
28. R. Vivek, R. Thangam, K. Muthuchelian, P. Gunasekaran, and K. S. Kaveri Kannan (2012). *Process. Biochem.* **47**, 2405–2410.
29. K. Gopinath, S. Gowri, and A. Arumugam (2013). *J. Nano Chem.* **3**, 68–75.
30. D. Wei, W. Sun, W. Qian, Y. Ye, and X. Ma (2009). *Carbohydr. Res.* **344**, 2375–2382.
31. S. Dudonne, X. Vitrac, P. Coutiere, M. Woillez, and J. M. Merillon (2009). *J. Agric. Food Chem.* **57**, 1768–1774.
32. I. Skandrani, J. Boubaker, W. Bhouri, I. Limem, S. Kilani, M. Ben Sghaier, A. Neffati, I. Bouhlel, K. Ghedira, and L. Chekir-Ghedira (2010). *Drug Chem. Toxicol.* **33**, 20–27.
33. I. Skandrani, I. Limem, A. Neffati, J. Boubaker, M. Ben Sghaier, W. Bhouri, I. Bouhlel, S. Kilani, K. Ghedira, and L. Chekir-Ghedira (2010). *Food Chem. Toxicol.* **48**, 710–715.
34. C. S. Moody and H. M. Hassan (1982). *Proc. Natl. Acad. Sci. U S A* **79**, 2855–2859.
35. H. M. Hassan and I. Fridovich (1979). *J. Biol. Chem.* **254**, 10846–10852.
36. C. E. Schwartz, J. Krall, L. Norton, K. McKay, D. Kay, and R. E. Lynch (1983). *J. Biol. Chem.* **258**, 6277–6281.
37. H. Rosen and S. J. Klebanoff (1979). *J. Exp. Med.* **149**, 27–39.
38. G. Applerot, A. Lipovsky, R. Dror, N. Perkas, Y. Nitzan, and R. Lubart (1968). *Adv. Funct. Mater.* **19**, 842–852.
39. K. J. A. Davies (1968). *J. Biol. Chem.* **262**, 9895–9901.
40. J. M. Gutteridge, D. A. Rowley, and B. Halliwell (1981). *Biochem. J.* **199**, 263–265.
41. R. L. Baldwin (1968). *J. Dairy Sci.* **51**, 104–111.
42. F. Regoli, M. Nigro, S. Bompadre, and G. W. Winston (2000). *Aquat. Toxicol.* **49**, 13–25.
43. C. S. Ryu, C. H. Kim, S. Y. Lee, K. S. Lee, K. J. Choung, G. Y. Song, B. H. Kim, S. Y. Ryu, H. S. Lee, and S. K. Kim (2012). *Food Chem.* **132**, 333–337.
44. S. Banerjee, J. P. Saikia, A. Kumar, and B. K. Konwar (2010). *Nanotechnology* **21**, 045101–045108.
45. G. Kiran, M. Sarangapani, T. Gouthami, and A. R. Narsimha Reddy (2013). *Toxic. Environ. Chem.* **95**, 367–378.
46. K. Gopinath, M. Chinnadurai, N. P. Devi, K. Bhakyaraj, S. Kumaraguru, T. Baranisri, A. Sudha, M. Zeeshan, A. Arumugam, M. Govindarajan, and N. S. Alharbi (2017). *J. Clust. Sci.* **28**, 621–635.
47. J. Ching, T. K. Chua, L. C. Chin, A. J. Lau, Y. K. Pang, J. M. Jaya, C. H. Tan, and H. L. Koh (2010). *Indian J. Exp. Biol.* **48**, 275–279.
48. R. Vidhya and R. Udayakumar (2015). *Int. J. Biochem. Res. Rev.* **7**, 192–203.
49. F. Nikkon, K. A. Salam, T. Yeasmin, A. Mosaddik, P. Khondkar, and M. E. Haque (2010). *Pharm. Biol.* **48**, 264–268.
50. G. Ramkumar, S. Karthi, R. Muthusamy, P. Suganya, D. Natarajan, E. J. Kweka, and M. S. Shivakumar (2016). *PLoS ONE* **11**, 1–11.